JOC The Journal of Organic Chemistry

Article

pubs.acs.org/joc

Synthesis of 2-Azulenyltetrathiafulvalenes by Palladium-Catalyzed Direct Arylation of 2-Chloroazulenes with Tetrathiafulvalene and Their Optical and Electrochemical Properties

Taku Shoji,*[,†] Takanori Araki,[†] Shuhei Sugiyama,[†] Akira Ohta,[†] Ryuta Sekiguchi,[‡] Shunji Ito,[‡] Tetsuo Okujima,[§] and Kozo Toyota[∥]

[†]Graduate School of Science and Technology, Shinshu University, Matsumoto 390-8621, Japan

[‡]Graduate School of Science and Technology, Hirosaki University, Hirosaki 036-8561, Japan

[§]Department of Chemistry and Biology, Graduate School of Science and Engineering, Ehime University, Matsuyama 790-8577, Japan

[∥]Department of Chemistry, Graduate School of Science, Tohoku University, Sendai 980-8578, Japan

Supporting Information

ABSTRACT: Tetrathiafulvalene (TTF) derivatives with 2-azulenyl substituents **5**−**11** were prepared by the palladium-catalyzed direct arylation reaction of 2-chloroazulenes with TTF in good yield. Photophysical properties of these compounds were investigated by UV−vis spectroscopy and theoretical calculations. Redox behavior of the novel azulene-substituted TTFs was examined by using cyclic voltammetry and differential pulse voltammetry, which revealed their multistep electrochemical oxidation and/or reduction properties. Moreover, these TTF derivatives showed significant spectral change in the visible region under the redox conditions.

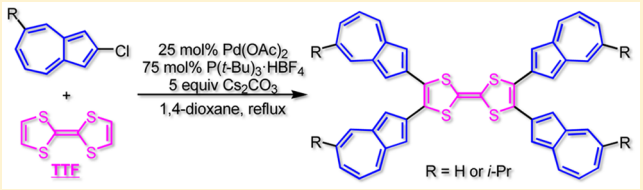

INTRODUCTION

Tetrathiafulvalene (TTF) and its derivatives have drawn attention as a component of organic electronic materials, such as molecular conductive materials based on their specific redox properties to form stabilized radical cationic and dicationic species by stepwise oxidation of one or both of the two 1,3-dithiole rings. Therefore, there are many reports concerning the preparation and properties of the TTF derivatives.[1]

Azulene derivatives have attracted the attention of many research groups because of its unique properties.[2] As similar to the TTF derivatives, azulene derivatives have also attracted the attention to their application for organic electronic materials.[3] However, there are few reports for the preparation and properties of azulene-fused and/or azulene-contained TTF derivatives in the literatures.[4] Only one example for the synthesis of azulene-substituted TTF derivative, i.e., 1,3-di(tetrathiafulvalenyl)azulene, has been reported by Iyoda et al.[5]

π-Electron systems with multiple 2-azulenyl substituents show a variety of properties, such as liquid crystallinity[6] and electrochromic behaviors.[7] Furthermore, these molecules have been expected to solar cell[8] and organic field effect transistor (OFET) applications.[3f,i,9] Therefore, development of an efficient synthetic method for the TTF derivatives with 2-azulenyl groups should contribute to the construction of organic materials with both specific features, such as amphoteric redox behavior and electrochromic property, of azulene and TTF derivatives. Previously, we have reported several synthetic procedures for 2-arylazulenes by palladium (Pd) catalyzed cross-coupling (e.g., Suzuki−Miyaura and Stille coupling reaction, and so on) of 2-haloazulene and/or 2-azulenyl metal reagents. The azulenyl metal reagents were useful for the construction of extended π-electron systems having 2-azulenyl groups. However, preparation of the azulenyl metal reagents for the cross-coupling reactions sometimes causes difficulty because of the limitation of the synthetic method that could be applied to the azulene derivatives. For instance, preparation of 2-(tributylstannyl)azulene by Pd-catalyzed stannylation is not effective owing to the homocoupling of the starting azulene derivative to form 2,2′-biazulene as a major product,[10] although the methodology is successful for the preparation of positional isomer at the 6-position.[11] Moreover, 2-azulenylborane reagent is revealed as to be relatively unstable and undergoes hydrolysis readily to afford its hydrocarbon derivative.[12] We have also reported an efficient synthetic procedure for the preparation of 2-aryl- and 2-heteroarylazulenes by the reaction of haloazulene with aryl- and heteroarylmagnesiumate complex, which was prepared from the corresponding aryl and heteroaryl halides.[13] However, the procedure also requires the synthetically troublesome 2-iodoazulene.[6b]

Received: November 24, 2016
Published: January 17, 2017

DOI: 10.1021/acs.joc.6b02818
J. Org. Chem. 2017, 82, 1657−1665

Scheme 1. Synthesis of 2-AzulenylTTFs, 5 and 7, and Bis(2-azulenyl)TTFs, 6syn, 6anti, 8syn, and 8anti

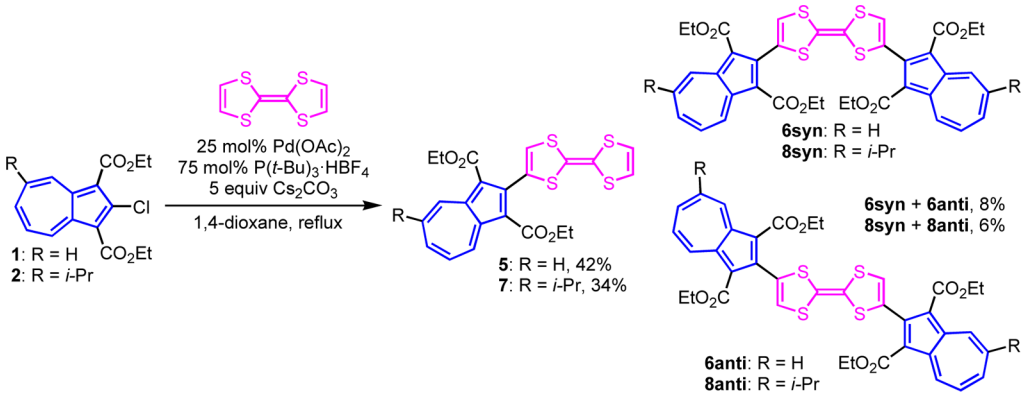

Scheme 2. Synthesis of tetra(2-Azulenyl)TTFs 9 and 10

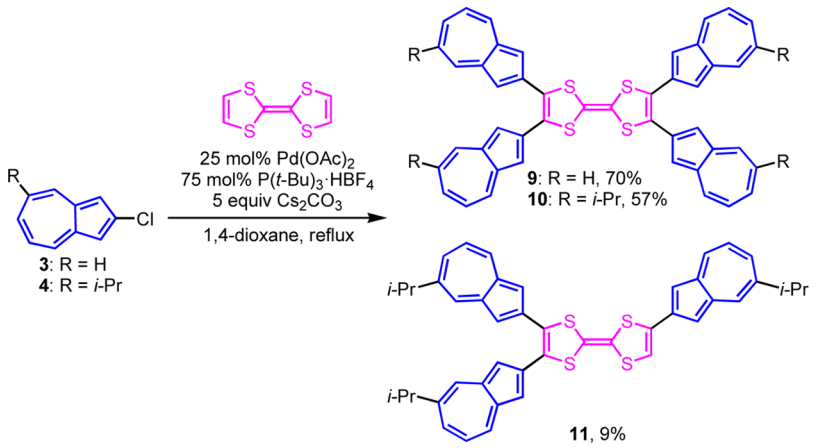

In recent years, direct arylation using a transition metal catalyst has attracted attention as a next generation cross-coupling reaction, because the procedure does not require organometallic reagents as a coupling partner.[14] In azulene chemistry, Pd-catalyzed direct cross-coupling have also been reported by several groups for the preparation of various arylazulene derivatives.[15] Although the direct coupling reaction with TTF should become one of the effective procedures, the synthesis of azulenyl TTF derivatives by direct arylation has never been reported, so far. Recently, Yorimitsu and co-workers have reported an efficient synthesis of TTF derivatives with multiple aryl substituents by the direct arylation of TTF with aryl bromides.[16] Thus, we have decided to apply the procedure reported by them to establish an efficient synthesis of TTF derivatives with 2-azulenyl groups.

Herein, we describe an efficient synthetic procedure for TTF derivatives with 2-azulenyl substituents **5**−**11** by the Pd-catalyzed direct arylation reaction of 2-chloroazulenes with TTF. Photophysical properties of the new TTF derivatives obtained by the cross-coupling reaction were clarified by absorption spectroscopy and theoretical calculations. The electrochemical behavior of the products was investigated by cyclic voltammetry (CV), differential pulse voltammetry (DPV), and spectroelectrochemistry.

RESULTS AND DISCUSSION

Synthesis. Azulene derivatives **1**−**4** were prepared from 2-amino-1,3-bis(ethoxycarbonyl)azulenes by 2 step procedures reported by Nozoe et al.[17] TTF derivatives with 2-azulenyl substituents **5**−**11** were prepared by Pd-catalyzed direct arylation of the corresponding 2-chloroazulenes **1**−**4** with TTF under the conditions reported by Yorimitsu et al.[15] To obtain the TTF derivatives with 2-azulenyl substituents, cross-coupling reaction of 2-chloroazulenes **1**−**4** (5 equiv. vs TTF) with TTF was examined in the presence of $Pd(OAc)_2$ (25 mol %), $P(t\text{-}Bu)_3{\cdot}HBF_4$ (75 mol%), and Cs_2CO_3 (5 equiv) as a catalytic system in 1,4-dioxane at the reflux temperature. Reaction of **1** with TTF in the presence of the Pd-catalyst, followed by chromatographic purification gave **5** in 42% yield, along with a mixture of **6syn** and **6anti** (ratio of syn:anti = 1:1 based on ^1H NMR) in 8% yield (Scheme 1). These results indicate that the second addition of 2-azulenyl group is not affected by the 2-azulenyl group introduced to the 1,3-dithiole unit. Separation of **6syn** and **6anti** was examined by recrystallization, reversed-phase chromatography, and gel permeation chromatography. However, all our attempts to separate these products resulted in a failure due to the similarity in their polarity and molecular structure. A similar Pd-catalyzed reaction of **2**[18] with TTF afforded **7** in 34% yield with a mixture of **8syn** and **8anti** (ratio of syn:anti = 1:1 based on ^1H NMR) in 6% yield (Scheme 1). The reaction was also carried out with a large excess of **1** and **2**, but the reaction did not give the presumed tri- and tetra(2-azulenyl)TTFs at all.

For the purpose of the preparation of 2-azulenylTTF derivatives without the two ester functions at their 1,3-positions, cross-coupling reaction of 2-chloroazulenes **3** and **4** with TTF was investigated under the similar reaction conditions of those for **1** and **2** (Scheme 2). Difference in

DOI: 10.1021/acs.joc.6b02818
J. Org. Chem. 2017, 82, 1657−1665

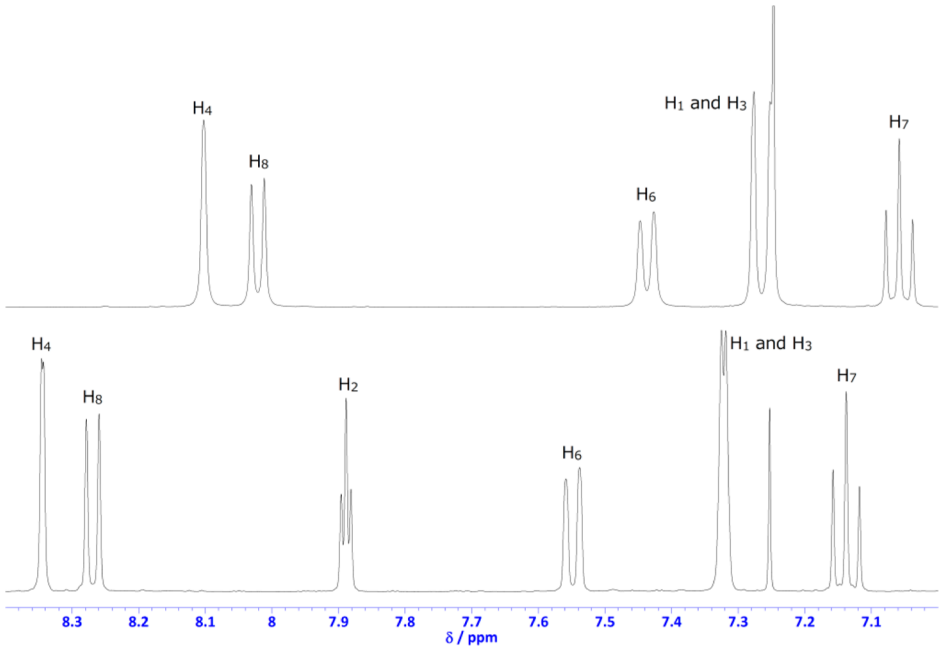

Figure 1. ^{1}H NMR spectra (500 MHz) of **10** (top) and **12** (bottom) in $CDCl_3$.

the reaction of **3** and **4** from the results on **1** and **2** was the formation of tetra(2-azulenyl)TTFs **9** and **10** in good yields. These results should be reasonably explained by the steric hindrance of the two ester groups on **1** and **2**, which prevent the formation of tri- and tetra(2-azulenyl)TTFs by the further cross-coupling reaction with **6syn**, **6anti** and **8syn**, **8anti**. Tetra(2-azulenyl)TTF **9** was obtained in 70% yield by the reaction of **3** with TTF in the presence of the Pd-catalyst. HRMS of compound **9** ionized by MALDI-TOF showed the correct molecular ion peaks, but NMR measurement of **9** was hampered by the less solubility in the common organic solvents. On the other hand, cross-coupling reaction of **4** with TTF afforded tetrakis(5-isopropyl-2-azulenyl)TTF (**10**) with considerable solubility in 57% yield, along with tris(5-isopropyl-2-azulenyl)TTF (**11**) in 9% yield. High solubility of **10** and **11** might be ascribed to less effective $\pi-\pi$ stacking of the molecules because of the steric hindrance of the isopropyl groups on azulene rings at the 5-position. We have also examined the direct arylation reaction of **1**−**4** with TTF using $PdCl_2(PPh_3)_2$ and $Pd(PPh_3)_4$ as a catalyst, but the attempts resulted into the recovery of starting materials, quantitatively. Therefore, electron-rich P(*t*-Bu)$_3$ ligand, which should promote the oxidative addition of the Pd-catalyst, is essential for the success of the reaction, because aryl chlorides are less reactive toward cross-coupling reactions rather than aryl bromides and iodides.[19]

Spectroscopic Properties. These new compounds were fully characterized on the basis of their spectral data, as summarized in the Experimental Section. HRMS of compounds **5**−**11** ionized by MALDI-TOF showed the expected molecular ion peaks. These results show the correctness of the structure of new compounds. The single crystal X-ray analysis may provide a useful packing information in the crystals for the design of organic electronic materials, but we could not obtain suitable single crystals of these compounds for the analysis, so far.

We tried the assignment of proton signals for the syn and anti structures of **6syn** and **6anti** (**8syn** and **8anti**) by using COSY experiments. Since the proton signals in ^{1}H NMR spectra displayed almost same chemical shifts, the assignment of **6syn** and **6anti** (**8syn** and **8anti**) was hampered by the similarity of their structures.

The ^{1}H NMR spectra of tetra(2-azulenyl)TTF (**10**) and 5-isopropylazulene (**12**) in $CDCl_3$ are compared in Figure 1. Upfield shifts for all ring protons of the azulene moiety in **10** were observed in $CDCl_3$ compared with those of **12**.[20] These results should reflect the both anisotropy derived from ring current effect of azulene rings and electron-donating nature of the TTF core.

UV−vis spectra of **7**, **8**, **10**, and **11** in CH_2Cl_2 are shown in Figure 2. Absorption maxima and coefficients (log ε) of **5**−**8**, **10**, and **11** are represented in the Experimental Section. The UV−vis spectra of TTF derivatives with 2-azulenyl substituents **5**−**8**, **10**, and **11** in the visible region showed a weak absorption band in CH_2Cl_2. The extinction coefficient of the absorption band was increased with the number of substituted azulene rings, because of the overlap of the transition of the azulene

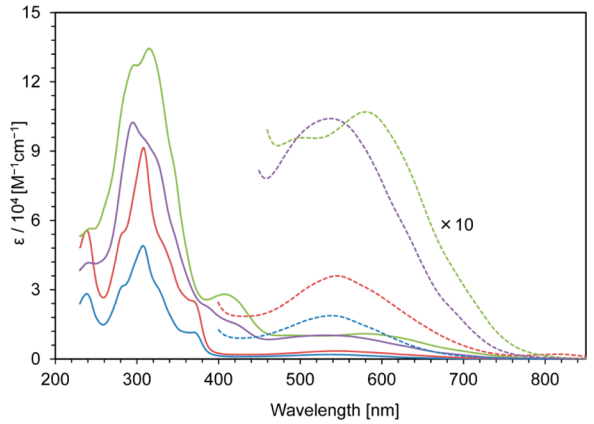

Figure 2. UV−vis spectra of **7** (blue line), **8** (red line), **10** (green line), and **11** (purple line) in CH_2Cl_2.

DOI: 10.1021/acs.joc.6b02818
J. Org. Chem. 2017, 82, 1657−1665

moieties. Compound **5** displayed an absorption band at λ_{max} = 537 nm in CH_2Cl_2. The longest wavelength absorption band of **6** (λ_{max} = 547 nm) exhibited a slight bathochromic shift compared with that of **5** and the azulene counterpart **13**[14b] (λ_{max} = 505 nm, Chart 1). This reflected the effective expansion of the π-electron system in **6** by the conjugation between the two 2-azulenyl groups through the TTF moiety.

Chart 1. Structure and Numbering of 5-Isopropylazylene (12) and 1,3-Bis(ethoxycarbonyl)azulene (13)

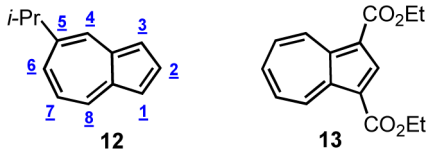

Absorption bands of compound **6** should become a superposition of two absorption spectra arising from a mixture of the syn and anti isomers **6syn** and **6anti**, but broad absorption band was exhibited in the visible region on the UV−vis spectrum. This result exhibits the similarity of the absorption spectra of compounds **6syn** and **6anti**, since the structure difference is only in their substitution patterns.

Similar with the relationship between **5** and **6**, absorption coefficient of **8** (λ_{max} = 546 nm) was almost twice as large as that of **7** (λ_{max} = 538 nm), as expected by the presence of two 2-azulenyl units in the molecule (Figures S32 and S35). Absorption maximum of **10** (λ_{max} = 581 nm) also exhibited a bathochromic shift relative to that of **5**−**8** and **11** (λ_{max} = 537 nm), owing to the further expansion of the π-electron system by four 2-azulenyl units on the TTF core.

To obtain further aspects for the spectroscopic properties, molecular orbital calculations were performed on **5**, **6syn**, **6anti**, **10**, and **11**, in which isopropyl group was replaced by hydrogen, using time-dependent density functional theory (TD-DFT) at the B3LYP/6-31G** level (Table S1).[21] The TTF moiety of **5**, **6syn**, and **6anti** in the optimized structures slightly twisted about the two 1,3-dithiole rings, as similar to that of diaryl TTFs and tetra-aryl TTFs observed by single-crystal X-ray analysis.[15] TD-DFT calculations of **5**, **6syn**, and **6anti** suggested that absorption bands in the visible region were assignable to the overlap of π−π^* transitions of the substituted azulene itself and ICT between 2-azulenyl groups and TTF core (see Table S1 and Figures S50−S52). Since the spectra of **6syn** and **6anti** obtained by the theoretical calculations displayed almost equal values, the broad absorption band of **6** in the visible region was explained by an overlap of transitions arising from that of two isomers **6syn** and **6anti**. Calculated HOMO−LUMO gap of **6syn** (1.97 eV) and **6anti** (2.00 eV) was lower than that of **5** (2.05 eV). Thus, the TTF moiety in **6syn** and **6anti** should contribute to decrease in the HOMO−LUMO gap, which exhibit the effectiveness of the conjugation between the two 2-azulenyl groups, although the TTF core takes a twisted form about the two 1,3-dithiole rings.

As shown in the Supporting Information, the HOMOs and LUMOs of **10** showed a symmetrical orbital reflecting the symmetrical structure (Figure S53). The broad absorption band

Table 1. Redox Potentials[a,b] of 2-Azulenyl TTF Derivatives 5−8, 10, 11, and the Parent TTF as a Reference Compound

sample	method[c]	E_1^{ox} [V]	E_2^{ox} [V]	E_3^{ox} [V]	E_1^{red} [V]	E_2^{red} [V]
TTF	CV	+0.11	+0.51			
	(DPV)	(+0.09)	(+0.49)			
5	CV	+0.05	+0.48			
		(E_{pa} = +0.11)	(E_{pa} = +0.56)		(E_{pc} = −1.42)	
		(E_{pc} = −0.02)	(E_{pc} = +0.41)			
	(DPV)	(+0.03)	(+0.46)	(+1.45)	(−1.37)	
6	CV	+0.03	+0.49			
		(E_{pa} = +0.08)	(E_{pa} = +0.56)		(E_{pc} = −1.42)	
		(E_{pc} = −0.03)	(E_{pc} = +0.43)			
	(DPV)	(+0.01)	(+0.47)	(+1.45)	(−1.38)	
7	CV	+0.03	+0.46			
		(E_{pa} = +0.06)	(E_{pa} = +0.50)		(E_{pc} = −1.48)	
		(E_{pc} = −0.01)	(E_{pc} = +0.41)			
	(DPV)	(+0.01)	(+0.44)	(+1.38)	(−1.44)	(−1.83)
8	CV	0.00	+0.47			
		(E_{pa} = +0.04)	(E_{pa} = +0.51)		(E_{pc} = −1.49)	
		(E_{pc} = −0.03)	(E_{pc} = +0.43)			
	(DPV)	(−0.02)	(+0.45)	(+1.38)	(−1.44)	(−1.91)
10	CV	+0.08			−1.59	
		(E_{pa} = +0.15)			(E_{pc} = −1.65)	
		(E_{pc} = 0.00)			(E_{pa} = −1.51)	
	(DPV)	(+0.06)	(+0.44)	(+0.87)	(−1.58)	(−1.84)
11	CV	+0.08			−1.57	
		(E_{pa} = +0.13)			(E_{pc} = −1.64)	
		(E_{pc} = +0.03)			(E_{pa} = −1.50)	
	(DPV)	(+0.06)	(+0.40)	(+0.62)	(−1.56)	(−1.78)

[a]V vs $Ag/AgNO_3$, 1 mM in benzonitrile containing Et_4NClO_4 (0.1 M), Pt electrode (internal diameter: 1.6 mm), and internal reference (Fc/Fc^+ = +0.15 V). In the cases of reversible waves, redox potentials measured by CV are presented. The peak potentials measured by DPV are shown in parentheses. [b]Half-wave potentials $E = (E_{pc} + E_{pa})/2$ on CV, E_{pc} and E_{pa} correspond to the cathodic and anodic peak potentials, respectively. [c]Scan rate: CV = 100 mV s^{-1}, DPV = 20 mV s^{-1}.

DOI: 10.1021/acs.joc.6b02818
J. Org. Chem. 2017, 82, 1657−1665

of **10** in the visible region could be assigned to the overlap of some transitions originated from the HOMOs located on both TTF and azulene moieties to the LUMOs mainly located on the azulene rings (Figure S53). Thus, the broad absorption band of **10** also could be concluded to the overlap of ICT transitions from TTF to the azulene moieties and $\pi-\pi^*$ transitions of the substituted azulene itself.

When the UV−vis spectra was measured in the presence of DDQ (5×10^{-3} M DDQ in CH_2Cl_2), 2-azulenylTTF derivatives **5**−**8** showed broad and relatively strong absorption bands in the visible region, which might be attributable to the generation of radical cationic species by one-electron oxidation of the TTF moiety. Compound **5** (λ_{max} = 589 nm) exhibited a bathochromic shift with 5×10^{-3} M DDQ in CH_2Cl_2 compared to that in CH_2Cl_2 (λ_{max} = 547 nm) (Figure S26). Similar bathochromic shift was also observed for that of the other 2-azulenylTTF derivatives with 5×10^{-3} M DDQ in CH_2Cl_2. Compound **6** exhibited broad absorption bands with three-peaks at λ_{max} = 457, 546, and 588 nm, when the UV−vis spectrum was measured with 5×10^{-3} M DDQ in CH_2Cl_2 (Figure S29). UV−vis spectrum of **7** (λ_{max} = 413, 450, and 540 nm) and **8** (λ_{max} = 545, 588, and 650 (sh) nm) also displayed the broad absorptions with several peaks in the presence of 5×10^{-3} M DDQ in CH_2Cl_2 (Figures S32 and S35). However, UV−vis spectrum of **10** and **11** in CH_2Cl_2 did not show the significant spectral changes by the addition of 5×10^{-3} M DDQ (Figures S38 and S41).

Recently, several groups have reported that some azulene derivatives with extended π electron systems exhibit fluorescence under acidic conditions, due to the emission from the protonated species of the azulene ring.[7,22] We also tried the measurement of fluorescence spectrum of 2-azulenylTTFs **5**−**8**, **10**, and **11** in both neutral and acidic solvent. However, no fluorescence was observed under the measurement conditions as similar to that of usual azulene derivatives.

Electrochemistry. It is well-known that the redox potentials of TTF derivatives depend on the substituents on the 1,3-dithiole ring.[23] Thus, to clarify the substituent effect of 2-azulenyl groups on the TTF core toward the electrochemical properties, we have examined the redox behavior of **5**−**8** and **10** by CV and DPV. The redox potentials (in volts vs Ag/Ag^+) of **5**−**8** and **10** measured by CV and DPV methods are summarized in Table 1.

As similar to the parent TTF, electrochemical oxidation of mono- and bis(1,3-diethoxycarbonyl-2-azulenyl)TTFs **5**−**8** on CV exhibited a two-stage wave due to the formation of radical cationic and dicationic species by the two-step oxidation of the TTF moiety. The first oxidation potential of these compounds are slightly varied to each other, although 1-azulenyl TTF derivative was reported to show almost same potential with the parent TTF.[5] 2-Azulenyl TTF derivative **5** showed the oxidation waves at +0.05 V and +0.48 V as half wave potentials on CV (Figure 3). Since the first oxidation potential of **5** was decreased by the substitution relative to that of the parent TTF (+0.11 V), we could conclude the π-conjugation is efficiently expanded by the 2-azulenyl group on TTF.

Further decrease in the first oxidation potential was observed in **6** (+0.03 V), which should indicate the extension of the π-electron system by the two 2-azulenyl units on TTF (Figure S45). Although the compound **6** exists as a mixture of syn and anti isomers, the first oxidation wave is reasonably explained by the oxidation of both regioisomers, since the DFT calculations revealed the equal HOMO levels of the isomers **6syn** and **6anti** (−4.67 eV). As similar to the results on **5** and **6**, quasi-reversible redox waves were observed by the electrochemical oxidation of **7** and **8**, which could also be ascribed to the formation of dicationic species by stepwise oxidation of the TTF moiety. TTF derivative **7** exhibited two quasi-reversible oxidation waves with potentials at +0.03 V and +0.46 V (Figure S46). The electrochemical oxidation of **8** also represented two quasi-reversible oxidation waves at 0.00 V and +0.47 V on CV (Figure S47). The first oxidation potential of **7** and **8** was slightly less nobler than that of **5** and **6**, respectively. This indicates increment of the HOMO level by electron-donating inductive effect of the isopropyl group on the azulene ring at 5-position. The two-step oxidation of tetra(2-azulenyl)TTF **10** (+0.06 V and +0.44 V) and tri(2-azulenyl)TTF **11** (+0.06 V and +0.40 V) was observed by DPV due to the stepwise formation of radical cationic and dicationic species (Figure S48 and S49). However, on CV of **10** and **11** we could observe only one quasi-reversible wave under the electrochemical oxidation conditions, because of overlapping of the second wave with the following irreversible waves. Thus, **10** and **11** are expected to be instable toward the electrochemical oxidation, rather than **5**−**8** with ethoxycarbonyl groups at the 1,3-positions. Therefore, less spectral changes of **10** and **11** in the presence of 5×10^{-3} M DDQ in CH_2Cl_2 might be ascribed to the instability of radical cationic state generated by the oxidation of the TTF moiety. Since the potential difference $E_2^{ox} - E_1^{ox}$ of **5**−**11** (0.34−0.46 V) is almost similar to that of the parent TTF (0.40 V), Coulombic repulsion between the two cations generated in the two 1,3-dithiole rings is not affected by the azulene substitution.

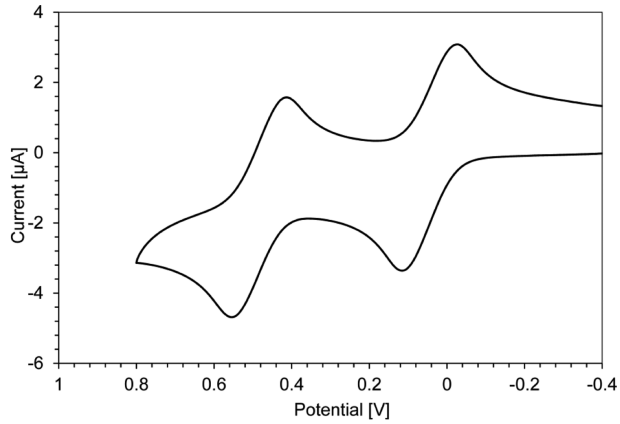

Figure 3. Cyclic voltammogram for oxidation of **5** (1 mM) in benzonitrile containing Et_4NClO_4 (0.1 M) as the supporting electrolyte; scan rate: CV = 100 mVs^{-1}.

The electrochemical reduction of tetra- and tri(2-azulenyl)-TTFs **10** and **11** showed a one-stage quasi-reversible wave on CV because of the reduction of azulene rings, although the reduction wave of **5**−**8** was irreversible. Previously, we have reported poly(2-azulenyl)benzene derivatives shows a reversible one or two-stage wave under the electrochemical reduction conditions.[9] In that study we have revealed that the multiple 2-azulenyl substituents on benzene ring increase the multiplicity of electron affinity due to the reduction of the respective azulene rings. Thus, in the cases of the reduction of **10** and **11** generation of stabilized anionic species $\mathbf{10}_{RED}^{4-}$ and $\mathbf{11}_{RED}^{3-}$ by the stepwise reduction as illustrated in Scheme 3 could be concluded.

DOI: 10.1021/acs.joc.6b02818
J. Org. Chem. 2017, 82, 1657−1665

Scheme 3. Presumed Redox Behavior of 10

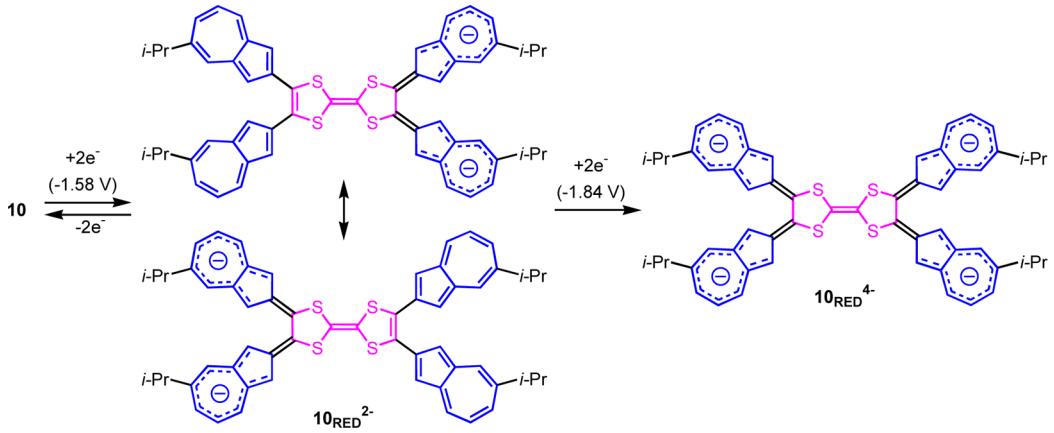

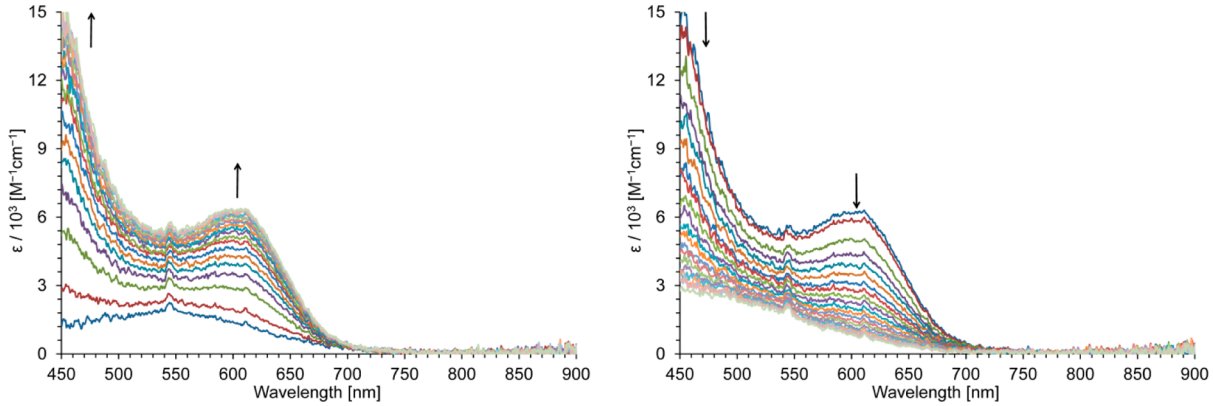

Figure 4. Continuous change in the UV/vis spectrum of **5**: constant-voltage electrochemical oxidation at +0.30 V (left) and further oxidation at +0.90 V (right) in benzonitrile containing Et_4NClO_4 (0.1 M) at 30 s intervals.

The first reduction potential of **5** (−1.37 V), **6** (−1.38 V), **7** (−1.44 V), and **8** (−1.44 V) determined by DPV analysis was less negative than that of **10** (−1.58 V) and **11** (−1.56 V). These results reflect that the electron-withdrawing ethoxycarbonyl substituent on the azulene ring directly affects to decrease the LUMO level of the molecules.

We have demonstrated the synthesis of various azulene-substituted, redox-active chromophores with the aim of creating stabilized electrochromic materials.[24] As a part of the study, we have reported 2-azulenyl groups connected by various π-electron systems induce electrochromic properties with high reversibility under the electrochemical reduction conditions, owing to the generation of stabilized anionic species.[6,8,9,12] However, in the previous cases irreversible spectral changes are observed under the electrochemical oxidation conditions, because of the instability of their cationic species formed by the electrolysis. Since the TTF derivatives with 2-azulenyl substituents **5**−**8** and **10** exhibited good reversibility in CV analysis, these compounds might become new examples of azulene-based redox system, which shows the electrochromic behavior under the electrochemical oxidation conditions. Therefore, to examine the electrochromic properties under the redox conditions, the spectral changes of the TTF derivatives with 2-azulenyl substituents **5**−**8**, **10**, and **11** were monitored by visible spectroscopy.[25]

Constant voltage oxidation of **5** at +0.30 V developed new absorption bands at around 450 and 605 nm in the visible region, which correspond to SOMO−LUMO and HOMO−SOMO transitions of the radical cationic species of the TTF derivative.[26] The spectrum is quite resembled to the spectrum of **5** measured in CH_2Cl_2 with 5×10^{-3} M DDQ. Thus, the spectral change indicates the generation of the same species with that formed by the addition of 5×10^{-3} M DDQ in CH_2Cl_2. These results should represent the formation of the radical cationic species $\mathbf{5}^{\cdot+}$ formed by one-electron oxidation of the TTF moiety. Reduction of the oxidized solution at −0.40 V regenerated the original spectrum of **5** almost completely. Thus, radical cationic species $\mathbf{5}^{\cdot+}$ is relatively stable under the measurement conditions. The new absorption bands of the radical cationic species $\mathbf{5}^{\cdot+}$ were decreased by further electrochemical oxidation at +0.90 V (Figure 4). Reverse reduction of the oxidized solution did not regenerate the original spectrum of **5**, although good reversibility in the two steps was observed by CV. The poor reversibility for the second spectral change of **5** should exhibit the less stability of the dicationic species $\mathbf{5}^{2+}$.

As similar to the results on **5**, the other TTF derivatives **6**, **7**, and **8** also displayed reversible electrochromism between neutral and radical cationic species, but irreversible with dicationic species. These results also indicate the dicationic species of **5**−**8** have less stability compared with their radical cationic species under the measurement conditions.

The absorption band in the visible region of **6** increased with the development of new absorption bands at around 450 and 620 nm under the constant voltage oxidation at +0.30 V. Reverse reduction at −0.40 V of the oxidized species decreased the new absorption bands, along with recovery of the original

DOI: 10.1021/acs.joc.6b02818
J. Org. Chem. 2017, 82, 1657−1665

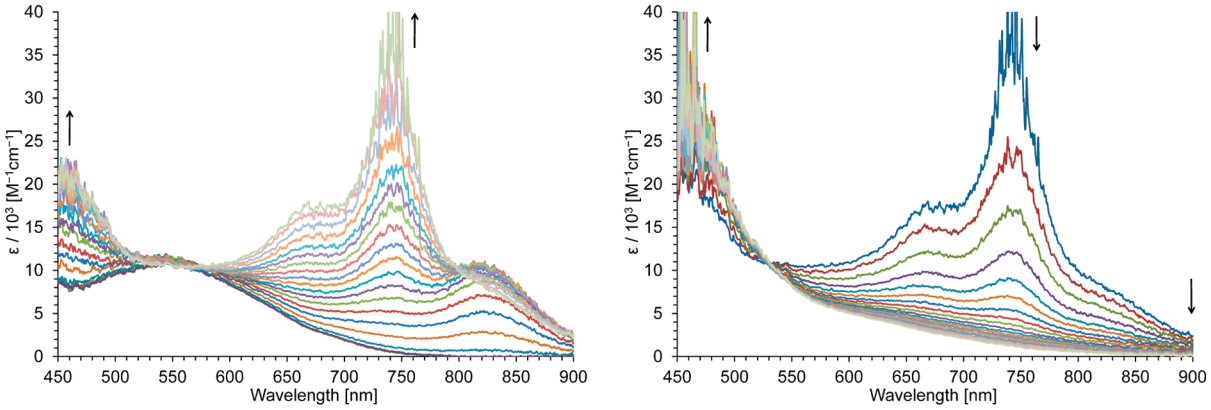

Figure 5. Continuous change in the visible spectrum of **11**: constant-voltage electrochemical reduction at −1.80 V (left) and reverse oxidation of the reduced species at 0.00 V (right) in benzonitrile containing Et_4NClO_4 (0.1 M) at 30 s intervals.

spectrum of **6** (Figure S30). A spectral change was observed in the visible spectra of **7**, which gradually developed new absorption bands originated from the radical cationic species on the TTF unit in the visible region at around 450 and 590 nm. On reverse reduction at −0.40 V, the new absorption in the visible region was decreased accompanying the regeneration of the parent absorption of **7** in the visible region (Figure S33). The visible spectrum of **8** was measured under the electrochemical oxidation conditions at +0.25 V. The absorption bands of **8** in the visible region gradually increased with the development of new absorption band (λ_{max} = 590 nm). As similar to **7**, reverse reduction at −0.40 V regenerated the original absorption bands of **8** (Figure S36). The longest wavelength absorption band of **10** and **11** slightly decreased during the electrochemical oxidation. However, the reversible reduction did not regenerate the spectrum of the corresponding starting compound (Figures S39 and S42). The irreversibility of the spectral changes indicates the instability of the oxidized species of **10** and **11** as observed in both UV−vis and CV analyses.

TTF derivatives **10** and **11** also showed spectral changes under the electrochemical reduction conditions, although the other derivatives did not exhibit the significant spectral changes. Particularly, when the spectral changes of **11** were monitored during the electrochemical reduction, new absorption bands at around 670 and 750 nm, which spread into the near-IR region, gradually developed probably due to the generation of anionic species. However, reverse oxidation did not reproduce the original spectrum of **11** (Figure 5).

CONCLUSIONS

In conclusion, we have established an efficient and direct synthetic method for 2-azulenylTTF derivatives **5**−**11**. 2-Chloroazulenes **1**−**4** reacted with TTF in the presence of $Pd(OAc)_2$, $P(t\text{-}Bu)_3{\cdot}HBF_4$, and Cs_2CO_3 as a catalytic system to afford the corresponding TTF derivatives with 2-azulenyl substituents **5**−**11**. Analyses by CV and DPV revealed a reversible two-stage oxidation properties of compounds **5**−**8** owing to the stepwise generation of radical cationic and dicationic species, although tetra(2-azulenyl)TTF **10** displayed a one-stage wave on CV. Reversible spectral change was also observed during the electrochemical oxidation conditions. TTF derivatives **5**−**8** exhibited significant spectral change with high reversibility, which is attributable to the formation of stabilized radical cationic species during the electrochemical reaction. In contrast to the results on **5**−**8**, tetra- and tri(2-azulenyl)TTFs **10** and **11** did not show reversibility in their electrochromic behavior due to the instability of their radical cationic species, as expected to the results obtained by UV−vis and CV analyses. Moreover, significant spectral change of compounds **10** and **11** was observed during the electrochemical reduction. In particular, tri(2-azulenyl)TTF **11** exhibited significant spectral change due to the generation of anionic species under the electrochemical reduction conditions.

The azulene system tends to stabilize both the cations and the anions, depending on the substitution position, by the contribution of the formal tropylium and cyclopentadienide substructures.[2] Substitution at the 1- and 3-positions on the azulenyl ring promotes an electron-donating nature, and on the other hand, azulen-4-yl, -6-yl, and -8-yl substituents have an electron-withdrawing property. Thus, TTF derivatives with 1-azulenyl or 6-azulenyl substituents should reveal the different character compared to the 2-azulenylTTF derivatives. Therefore, in order to evaluate the scope of this class of molecules examined by this study, the synthesis of mono-, di-, and tetra(1- and 6-azulenyl)TTF derivatives by the direct arylation and their properties are now in progress in our laboratory.

EXPERIMENTAL SECTION

General. ^1H and ^{13}C NMR spectra were measured at 500 MHz (^1H NMR) and 125 MHz (^{13}C NMR), respectively. Voltammetry measurements were carried out with Pt working and auxiliary electrodes and an Ag/Ag^+ reference electrode formed from $AgNO_3$ (0.01 M) in acetonitrile containing tetrabutylammonium perchlorate (0.1 M).

Reaction of 1 with TTF. To a solution of **1** (383 mg, 1.25 mmol), TTF (49 mg, 0.24 mmol), $P(t\text{-}Bu)_3{\cdot}HBF_4$ (60 mg, 0.21 mmol), and Cs_2CO_3 (409 mg, 1.26 mmol) in 1,4-dioxane (4 mL) was added $Pd(OAc)_2$ (20 mg, 0.089 mmol). The resulting mixture was refluxed for 37 h under an Ar atmosphere. The reaction mixture was poured into water and extracted with CH_2Cl_2. The organic layer was washed with brine, dried with Na_2SO_4, and concentrated under reduced pressure. The residue was purified by silica gel column chromatography with CH_2Cl_2/AcOEt (50:1) to give **5** (48 mg, 42%, purple crystals) and **6** (14 mg, 8%, purple crystals).

*2-(1,3-Dithiol-2-ylidene)-4-(1,3-diethoxycarbonyl-2-azulenyl)-1,3-dithiole (**5**).* mp 172−173 °C; IR (AT−IR): ν_{max} = 3070 (w), 2962 (w), 2926 (w), 1683 (m), 1595 (w), 1543 (w), 1519 (w), 1481 (m), 1462 (m), 1430 (s), 1382 (m), 1354 (w), 1335 (w), 1279 (w), 1238 (m), 1203 (m), 1182 (m), 1108 (m), 1043 (m), 1029 (m), 967 (w), 907 (w), 876 (w), 810 (m), 796 (m), 782 (m), 749 (w), 734 (w), 698 (w), 685 (w) cm^{-1}; UV−vis (CH_2Cl_2): λ_{max} (log ε) = 235 (4.50), 278 sh (4.49), 305 (4.71), 327 sh (4.47), 368 sh (4.00), 537 (3.28), 598 sh

DOI: 10.1021/acs.joc.6b02818
J. Org. Chem. 2017, 82, 1657−1665

(3.12) nm; UV−vis (5×10^{-3} M DDQ in CH_2Cl_2): λ_{max} (log ε) = 413 sh (3.77), 450 (4.03), 547 (3.71), 590 (3.74) nm; ^{1}H NMR (500 MHz, $CDCl_3$): δ_H = 9.69 (d, 2H, J = 10.0 Hz, $H_{4,8}$), 8.01 (t, 1H, J = 10.0 Hz, H_6), 7.77 (t, 2H, J = 10.0 Hz, $H_{5,7}$), 6.36 (m, 2H, H_{TTF}), 6.11 (br. s, 1H, H_{TTF}), 4.41 (q, 4H, J = 7.5 Hz, CO_2Et), 1.40 (t, 6H, J = 7.5 Hz, CO_2Et) ppm; ^{13}C NMR (125 MHz, $CDCl_3$): δ_C = 165.1, 144.2, 142.7, 141.4, 139.8, 130.9, 130.8, 119.2, 119.0, 117.8, 115.6, 111.6, 110.1, 60.7, 14.1 ppm; HRMS (MADLI−TOF): $C_{22}H_{18}O_4S_4^+$ $[M]^+$ 474.0083, found: 474.0077.

*2-[4- and 5-(1,3-Diethoxycarbonyl-2-azulenyl)-1,3-dithiol-2-ylidene]-4-(1,3-diethoxycarbonyl-2-azulenyl)-1,3-dithiole (**6**).* mp 272−274 °C; IR (AT−IR): ν_{max} = 3082 (w), 2979 (w), 2925 (w), 2362 (w), 1693 (m), 1669 (m), 1595 (w), 1532 (w), 1484 (w), 1455 (w), 1432 (s), 1411 (w), 1384 (m), 1357 (w), 1295 (w), 1254 (m), 1223 (m), 1198 (m), 1180 (m), 1125 (m), 1111 (m), 1055 (w), 1026 (w), 934 (w), 886 (w), 793 (m), 779 (w), 765 (w), 741 (w), 720 (w), 695 (w), 677 (w), 658 (s), 627 (w), 605 (w) cm^{-1}; UV−vis (CH_2Cl_2): λ_{max} (log ε) = 235 (4.78), 278 sh (4.72), 305 (4.98), 334 sh (4.66), 367 sh (4.34), 431 sh (3.28), 497 sh (3.43), 547 (3.52), 621 sh (3.36) nm; UV−vis (5×10^{-3} M DDQ in CH_2Cl_2): λ_{max} (log ε) = 457 (4.34), 546 (4.03), 588 (4.06), 652 sh (3.80) nm; ^{1}H NMR (500 MHz, $CDCl_3$): δ_H = 9.68−9.64 (m, 4H, $H_{4,8,4',8'}$), 8.01−7.95 (m, 2H, $H_{6,6'}$), 7.77−7.72 (m, 4H, $H_{5,7,5',7'}$), 6.09−6.08 (m, 2H, H_{TTF}), 4.44−4.38 (m, 8H, CO_2Et), 1.45−1.42 (m, 12H, CO_2Et) ppm; ^{13}C NMR (125 MHz, $CDCl_3$): δ_C = 165.1, 165.0, 142.69, 142.66, 141.45, 141.43, 139.8, 130.8, 130.7, 117.8, 116.1, 115.7, 60.70, 60.67, 14.3 ppm, some signals were overlapped with the other signals; HRMS (MADLI−TOF): Calcd for $C_{38}H_{32}O_8S_4^+$ $[M]^+$ 744.0975, found: 744.0977.

Reaction of 2 with TTF. To a solution of **2** (443 mg, 1.27 mmol), TTF (51 mg, 0.25 mmol), P(t-Bu)$_3$·HBF$_4$ (58 mg, 0.20 mmol), and Cs_2CO_3 (415 mg, 1.27 mmol) in 1,4-dioxane (5 mL) was added $Pd(OAc)_2$ (16 mg, 0.071 mmol). The resulting mixture was refluxed for 22 h under an Ar atmosphere. The reaction mixture was poured into water and extracted with CH_2Cl_2. The organic layer was washed with brine, dried with Na_2SO_4, and concentrated under reduced pressure. The residue was purified by silica gel column chromatography with CH_2Cl_2 to give **7** (44 mg, 34%, purple oil) and **8** (12 mg, 6%, purple crystal).

*2-(1,3-Dithiol-2-ylidene)-4-(1,3-diethoxycarbonyl-5-isopropyl-2-azulenyl)-1,3-dithiole (**7**).* IR (AT−IR): ν_{max} = 3069 (w), 2962 (w), 2926 (w), 1683 (s), 1595 (w), 1542 (w), 1519 (w), 1481 (w), 1462 (w), 1430 (s), 1382 (m), 1354 (w), 1335 (w), 1279 (w), 1237 (m), 1203 (s), 1182 (s), 1108 (m), 1043 (m), 1028 (m), 966 (w), 908 (w), 869 (w), 811 (m), 796 (m), 781 (m), 734 (w), 700 (w), 672 (w) cm^{-1}; UV−vis (CH_2Cl_2): λ_{max} (log ε) = 239 (4.45), 281 sh (4.49), 308 (4.69), 328 sh (4.47), 370 (4.06), 499 sh (3.19), 538 (3.27), 592 sh (3.10) nm; UV−vis (5×10^{-3} M DDQ in CH_2Cl_2): λ_{max} (log ε) = 413 (3.71), 450 (3.91), 540 (3.64), 586 (3.62) nm; ^{1}H NMR (500 MHz, $CDCl_3$): δ_H = 9.75 (d, 1H, J = 1.5 Hz, H_4), 9.56 (d, 1H, J = 10.0 Hz, H_8), 7.92 (d, 1H, J = 10.0 Hz, H_6), 7.70 (t, 1H, J = 10.0 Hz, H_7), 6.34−6.30 (m, 2H, H_{TTF}), 6.04 (s, 1H, H_{TTF}), 4.39−4.33 (m, 4H, CO_2Et), 3.25 (sept, 1H, J = 7.0 Hz, i-Pr), 1.42 (d, 6H, J = 7.0 Hz, i-Pr), 1.37 (q, 6H, J = 7.5 Hz, CO_2Et) ppm; ^{13}C NMR (125 MHz, $CDCl_3$): δ_C = 165.2, 165.1, 152.5, 144.4, 142.8, 142.7, 140.6, 139.5, 138.2, 131.2, 130.6, 119.2, 118.9, 116.6, 116.5, 115.1, 111.8, 109.8, 60.55, 60.52, 39.3, 24.7, 14.2, 14.1 ppm; HRMS (MALDI-TOF): Calcd for $C_{25}H_{24}O_4S_4^+$ $[M]^+$ 516.0552; found: 516.0544.

*2-[4- and 5-(1,3-Diethoxycarbonyl-5-isopropyl-2-azulenyl)-1,3-dithiol-2-ylidene]-4-(1,3-diethoxycarbonyl-5-isopropyl-2-azulenyl)-1,3-dithiole (**8**).* mp 248−249 °C; IR (AT−IR): ν_{max} = 3084 (w), 2962 (w), 2934 (w), 2903 (w), 1680 (s), 1598 (w), 1549 (w), 1518 (w), 1482 (w), 1463 (w), 1430 (s), 1405 (m), 1381 (m), 1352 (w), 1310 (w), 1279 (w), 1238 (s), 1201 (s), 1176 (m), 1125 (m), 1109 (m), 1045 (m), 1028 (m), 970 (w), 909 (w), 876 (w), 816 (m), 783 (w), 759 (w), 699 (w), 655 (w) cm^{-1}; UV−vis (CH_2Cl_2): λ_{max} (log ε) = 239 (4.75), 280 sh (4.73), 308 (4.96), 337 sh (4.66), 371 sh (4.39), 474 sh (3.35), 507 sh (3.48), 546 (3.56), 601 sh (3.43) nm; UV−vis (5×10^{-3} M DDQ in CH_2Cl_2): λ_{max} (log ε) = 419 (4.19), 457(4.41), 545 (4.11), 588 (4.14), 650 sh (3.89) nm; ^{1}H NMR (500 MHz, $CDCl_3$): δ_H = 9.75 (m, 2H, H_4), 9.56 (m, 2H, $H_{8,8'}$), 7.92 (m, 2H, $H_{6,6'}$), 7.70 (m, 2H, $H_{7,7'}$), 6.05 (br. s, 2H, H_{TTF}), 4.44−4.37 (m, 8H, CO_2Et), 3.30−3.23 (m, 2H, i-Pr), 1.46−1.41 (m, 24H, i-Pr, CO_2Et) ppm; ^{13}C NMR (125 MHz, $CDCl_3$): δ_C = 165.3, 165.2, 165.13, 165.08, 152.52, 152.49, 142.81, 142.77, 142.69, 142.66, 140.62, 140.61, 139.5, 138.2, 131.4, 131.1, 130.61, 130.58, 116.7, 115.6, 60.54, 60.51, 39.3, 24.7, 14.3 ppm; HRMS (MALDI-TOF): calcd for $C_{44}H_{44}O_8S_4^+$ $[M]^+$ 828.1914; found: 828.1918.

*Tetra(2-azulenyl)tetrathiafulvalene (**9**).* To a solution of **3** (207 mg, 1.27 mmol), TTF (51 mg, 0.25 mmol), P(t-Bu)$_3$·HBF$_4$ (57 mg, 0.20 mmol), and Cs_2CO_3 (417 mg, 1.28 mmol) in 1,4-dioxane (5 mL) was added $Pd(OAc)_2$ (18 mg, 0.08 mmol). The resulting mixture was refluxed for 23 h under an Ar atmosphere. The precipitated crystals were collected by filtration and washed with $CHCl_3$ to give **9** (124 mg, 70%) as insoluble green crystals. mp 240−241 °C (decomp.); IR (AT−IR): ν_{max} = 3050 (w), 1577 (m), 1532 (m), 1517 (m), 1488 (m), 1474 (m), 1401 (s), 1337 (w), 1305 (w), 1291 (w), 1269 (w), 1203 (w), 1177 (w), 1105 (w), 1024 (w), 992 (w), 978 (w), 939 (w), 894 (m), 849 (w), 813 (s), 781 (m), 734 (s), 682 (m), 665 (m), 656 (w), cm^{-1}; HRMS (MALDI-TOF): calcd for $C_{46}H_{28}S_4^+$ $[M]^+$ 708.1069, found: 708.1064; Anal. Calcd for $C_{46}H_{28}S_4$·1.15$CHCl_3$: C, 66.92; H, 3.47. Found: C, 66.83; H, 3.38.

Reaction of 4 with TTF. To a solution of **4** (277 mg, 1.36 mmol), TTF (51 mg, 0.25 mmol), P(t-Bu)$_3$·HBF$_4$ (56 mg, 0.19 mmol), and Cs_2CO_3 (412 mg, 1.26 mmol) in 1,4-dioxane (5 mL) was added $Pd(OAc)_2$ (14 mg, 0.062 mmol). The resulting mixture was refluxed for 48 h under an Ar atmosphere. The reaction mixture was poured into water and extracted with CH_2Cl_2. The organic layer was washed with brine, dried with Na_2SO_4, and concentrated under reduced pressure. The residue was purified by silica gel column chromatography with CH_2Cl_2 to give **10** (125 mg, 57%, green crystals) and **11** (16 mg, 9%, green crystals).

*2-[4,5-Bis(5-isopropyl-2-azulenyl)-1,3-dithiol-2-ylidene]-4,5-bis(5-isopropyl-2-azulenyl)-1,3-dithiole (**10**).* mp 223−225 °C; IR (AT−IR): ν_{max} = 2960 (w), 2925 (w), 2869 (w), 1579 (w), 1520 (m), 1486 (m), 1463 (m), 1406 (s), 1383 (w), 1362 (w), 1320 (w), 1255 (w), 1209 (w), 1131 (w), 1104 (w), 1035 (w), 1018 (w), 979 (w), 930 (w), 879 (w), 816 (s), 785 (m), 767 (m), 712 (w), 667 (w), 655 (w) cm^{-1}; UV−vis (CH_2Cl_2): λ_{max} (log ε) = 237 sh (4.74), 297 (5.11), 316 (5.13), 347 sh (4.91), 409 (4.45), 494 sh (3.98), 581 (4.03), 630 sh (3.93) nm; UV−vis (5×10^{-3} M DDQ in CH_2Cl_2): λ_{max} (log ε) = 409 (4.42), 506 sh (4.00), 610 sh (3.87) nm; ^{1}H NMR (500 MHz, $CDCl_3$): δ_H = 8.12 (s, 4H, H_4), 8.03 (d, 4H, J = 10.0 Hz, H_8), 7.45 (d, 4H, J = 10.0 Hz, H_6), 7.29 (s, 4H, H_1 or H_3), 7.27 (s, 4H, H_1 or H_3), 7.07 (t, 4H, J = 10.0 Hz, H_7), 3.03 (sept, 4H, J = 7.0 Hz, i-Pr), 1.34 (d, 24H, J = 7.0 Hz, i-Pr) ppm; ^{13}C NMR (125 MHz, $CDCl_3$): δ_C = 144.1, 141.0, 140.3, 139.9, 136.5, 136.3, 135.3, 128.6, 123.6, 116.8, 116.4, 38.6, 24.6 ppm, one signal is overlapped with the other signal; HRMS (MALDI-TOF): Calcd for $C_{58}H_{52}S_4^+$ $[M]^+$ 876.2946; found: 876.2949.

*2-[4,5-Bis(5-isopropyl-2-azulenyl)-1,3-dithiol-2-ylidene]-4-(5-isopropyl-2-azulenyl)-1,3-dithiole (**11**).* mp 150−152 °C; IR (AT−IR): ν_{max} = 2959 (w), 1578 (m), 1529 (m), 1484 (m), 1460 (m), 1442 (m), 1406 (s), 1362 (w), 1321 (w), 1261 (w), 1214 (w), 1141 (w), 1104 (w), 1035 (w), 975 (w), 929 (w), 883 (w), 848 (w), 808 (s), 776 (s), 720 (w), 705 (w), 684 (w), 673 (w) cm^{-1}; UV−vis (CH_2Cl_2): λ_{max} (log ε) = 241 (4.62), 296 (5.01), 321 sh (4.95), 387 sh (4.35), 423 sh (4.17), 537 (4.02) nm; UV−vis (5×10^{-3} M DDQ in CH_2Cl_2): λ_{max} (log ε) = 424 sh (4.18), 509 (4.01) nm; ^{1}H NMR (500 MHz, $CDCl_3$): δ_H = 8.19 (s, 1H, H_4), 8.13−8.11 (m, 3H, $H_{4',4''}$ and H_8), 8.05 (d, 2H, J = 10.0 Hz, $H_{8'}$ or $H_{8''}$), 8.03 (d, 2H, J = 10.0 Hz, $H_{8'}$ or $H_{8''}$), 7.46 (d, 3H, J = 10.0 Hz, $H_{6,6',6''}$), 7.29−7.25 (m, 6H, $H_{1,3,1',3',1'',3''}$), 7.15−7.05 (m, 3H, $H_{5,5',5''}$), 6.90 (s, 1H, H_{TTF}), 3.08−3.00 (m, 3H, i-Pr), 1.37−1.33 (m, 18H, i-Pr) ppm; ^{13}C NMR (125 MHz, $CDCl_3$): δ_C = 144.5, 144.1, 141.0, 140.9, 140.5, 140.3, 139.9, 136.5, 136.4, 136.0, 135.9, 135.3, 134.8, 133.6, 128.5, 128.4, 124.1, 123.6, 116.79, 116.76, 116.41, 116.37, 113.9, 113.5, 110.4, 109.2, 38.62, 38.58, 24.6 ppm; HRMS (MALDI-TOF): Calcd for $C_{45}H_{40}S_4^+$ $[M]^+$ 708.2007; found: 708.2008.

DOI: 10.1021/acs.joc.6b02818
J. Org. Chem. 2017, 82, 1657−1665

■ ASSOCIATED CONTENT

Supporting Information

The Supporting Information is available free of charge on the ACS Publications website at DOI: 10.1021/acs.joc.6b02818.

Copies of ^{1}H, ^{13}C NMR, COSY spectra; HRMS and UV−vis spectra; continuous change in the visible spectra; cyclic and differential pulse voltammograms of the new compounds; and Frontier Kohn−Sham orbitals of compounds **5**, **6syn**, **6anti**, **10**, and **11** (PDF)

■ AUTHOR INFORMATION

Corresponding Author

*E-mail: tshoji@shinshu-u.ac.jp

ORCID

Taku Shoji: 0000-0001-8176-2389

Notes

The authors declare no competing financial interest.

■ ACKNOWLEDGMENTS

This work was supported by JSPS KAKENHI Grant Number 25810019 (TS), JSPS KAKENHI Grant Number 16K05679 (SI), and JSPS KAKENHI Grant Number 26410052 (TO), and also by a research grant from the Faculty of Science, Shinshu University.

■ REFERENCES

(1) Special Issue on Molecular Conductors: Batail, P. *Chem. Rev.* **2004**, *104*, 4887−4890.

(2) Zeller, K.-P. Azulene. In *Methoden der Organischen Chemie (Houben-Weyl)*, 4th ed.; Kropf, H., Ed.; Thieme: Stuttgart, Germany, 1985; Vol. *V*, part 2c, pp 127−418.

(3) (a) Wang, F.; Lai, Y.-H. *Macromolecules* **2003**, *36*, 536−538. (b) Wang, F.; Lai, Y.-H.; Han, M. Y. *Org. Lett.* **2003**, *5*, 4791−4794. (c) Amir, E.; Amir, R. J.; Campos, L. M.; Hawker, C. J. *J. Am. Chem. Soc.* **2011**, *133*, 10046−10049. (d) Kitai, J.; Kobayashi, T.; Uchida, W.; Hatakeyama, M.; Yokojima, S.; Nakamura, S.; Uchida, K. *J. Org. Chem.* **2012**, *77*, 3270−3276. (e) Wang, F.; Lin, T. T.; He, C.; Chi, H.; Tang, T.; Lai, Y.-H. *J. Mater. Chem.* **2012**, *22*, 10448−10451. (f) Yamaguchi, Y.; Ogawa, K.; Nakayama, K.; Ohba, Y.; Katagiri, H. *J. Am. Chem. Soc.* **2013**, *135*, 19095−19098. (g) Yao, J.; Cai, Z.; Liu, Z.; Yu, C.; Luo, H.; Yang, Y.; Yang, S.; Zhang, G.; Zhang, D. *Macromolecules* **2015**, *48*, 2039−2047. (h) Nishimura, H.; Ishida, N.; Shimazaki, A.; Wakamiya, A.; Saeki, A.; Scott, L. T.; Murata, Y. *J. Am. Chem. Soc.* **2015**, *137*, 15656−15659. (i) Yamaguchi, Y.; Takubo, M.; Ogawa, K.; Nakayama, K.; Koganezawa, T.; Katagiri, H. *J. Am. Chem. Soc.* **2016**, *138*, 11335−11343.

(4) (a) Yamamoto, H. M.; Yamaura, J.; Kato, R. *J. Mater. Chem.* **1998**, *8*, 289−294. (b) Ohta, A.; Yamaguchi, K.; Fujisawa, N.; Yamashita, Y.; Fujimori, K. *Heterocycles* **2001**, *54*, 377−385. (c) Petersen, M. A.; Andersson, A. S.; Kilsa, K.; Nielsen, M. B. *Eur. J. Org. Chem.* **2009**, *2009*, 1855−1858. (d) Shoji, T.; Ito, S.; Okujima, T.; Morita, N. *Org. Biomol. Chem.* **2012**, *10*, 8308−8313.

(5) Iyoda, M.; Fukuda, M.; Yoshida, M.; Sasaki, S. *Chem. Lett.* **1994**, *23*, 2369−2372.

(6) (a) Ito, S.; Ando, M.; Nomura, A.; Morita, N.; Kabuto, C.; Mukai, H.; Ohta, K.; Kawakami, J.; Yoshizawa, A.; Tajiri, A. *J. Org. Chem.* **2005**, *70*, 3939−3949. (b) Nakagawa, K.; Yokoyama, T.; Toyota, K.; Morita, N.; Ito, S.; Tahata, S.; Ueda, M.; Kawakami, J.; Yokoyama, M.; Kanai, Y.; Ohta, K. *Tetrahedron* **2010**, *66*, 8304−8312. (c) Adachi, T.; Saitoh, H.; Yamamura, Y.; Hishida, M.; Ueda, M.; Ito, S.; Saito, K. *Bull. Chem. Soc. Jpn.* **2013**, *86*, 1022−1027.

(7) (a) Shoji, T.; Shimomura, E.; Maruyama, M.; Ito, S.; Okujima, T.; Morita, N. *Eur. J. Org. Chem.* **2013**, *2013*, 957−964. (b) Shoji, T.; Ito, S.; Okujima, T.; Morita, N. *Chem. - Eur. J.* **2013**, *19*, 5721−5730. (c) Shoji, T.; Maruyama, M.; Shimomura, E.; Maruyama, A.; Ito, S.; Okujima, T.; Toyota, K.; Morita, N. *J. Org. Chem.* **2013**, *78*, 12513−12524. (d) Shoji, T.; Maruyama, M.; Maruyama, A.; Ito, S.; Okujima, T.; Toyota, K. *Chem. - Eur. J.* **2014**, *20*, 11903−11912.

(8) Puodziukynaite, E.; Wang, H.-W.; Lawrence, J.; Wise, A. J.; Russell, T. P.; Barnes, M. D.; Emrick, T. *J. Am. Chem. Soc.* **2014**, *136*, 11043−11049.

(9) Yamaguchi, Y.; Maruya, Y.; Katagiri, H.; Nakayama, K.; Ohba, Y. *Org. Lett.* **2012**, *14*, 2316−2319.

(10) Ito, S.; Terazono, T.; Kubo, T.; Okujima, T.; Morita, N.; Murafuji, T.; Sugihara, Y.; Fujimori, K.; Kawakami, J.; Tajiri, A. *Tetrahedron* **2004**, *60*, 5357−5366.

(11) (a) Okujima, T.; Ito, S.; Morita, N. *Tetrahedron Lett.* **2002**, *43*, 1261−1264. (b) Ito, S.; Okujima, T.; Morita, N. *J. Chem. Soc., Perkin Trans. 1* **2002**, 1896−1905.

(12) Ito, S.; Kubo, T.; Morita, N.; Matsui, Y.; Watanabe, T.; Ohta, A.; Fujimori, K.; Murafuji, T.; Sugihara, Y.; Tajiri, A. *Tetrahedron Lett.* **2004**, *45*, 2891−2894.

(13) (a) Shoji, T.; Kikuchi, S.; Ito, S.; Morita, N. *Heterocycles* **2005**, *66*, 91−94. (b) Shoji, T.; Ito, S.; Toyota, K.; Iwamoto, T.; Yasunami, M.; Morita, N. *Eur. J. Org. Chem.* **2009**, *2009*, 4307−4315. (c) Shoji, T.; Maruyama, A.; Ito, S.; Okujima, T.; Yasunami, M.; Higashi, J.; Morita, N. *Heterocycles* **2014**, *89*, 2588−2603.

(14) (a) Dyker, G. *Angew. Chem., Int. Ed.* **1999**, *38*, 1698−1712. (b) Zhao, D.; Wang, W.; Yang, F.; Lan, J.; Yang, L.; Gao, G.; You, J. *Angew. Chem., Int. Ed.* **2009**, *48*, 3296−3300. (c) Xiao, B.; Fu, Y.; Xu, J.; Gong, T.-J.; Dai, J.-J.; Yi, J.; Liu, L. *J. Am. Chem. Soc.* **2010**, *132*, 468−469. (d) Schipper, D. J.; Fagnou, K. *Chem. Mater.* **2011**, *23*, 1594−1600. (e) Miura, M.; Satoh, T.; Hirano, K. *Bull. Chem. Soc. Jpn.* **2014**, *87*, 751−764.

(15) (a) Dyker, G.; Borowski, S.; Heiermann, J.; Körning, J.; Opwis, K.; Henkel, G.; Köckerling, M. *J. Organomet. Chem.* **2000**, *606*, 108−111. (b) Shoji, T.; Maruyama, A.; Araki, T.; Ito, S.; Okujima, T. *Org. Biomol. Chem.* **2015**, *13*, 10191−10197. (c) Murai, M.; Yanagawa, M.; Nakamura, M.; Takai, K. *Asian J. Org. Chem.* **2016**, *5*, 629−635.

(16) (a) Mitamura, Y.; Yorimitsu, H.; Oshima, K.; Osuka, A. *Chem. Sci.* **2011**, *2*, 2017−2021. (b) Ueno, R.; Fujino, D.; Yorimitsu, H.; Osuka, A. *Chem. - Eur. J.* **2013**, *19*, 7156−7161.

(17) Nozoe, T.; Seto, S.; Matsumura, S. *Bull. Chem. Soc. Jpn.* **1962**, *35*, 1990−1998.

(18) Morita, T.; Fujita, T.; Takase, K. *Bull. Chem. Soc. Jpn.* **1980**, *53*, 1647−1651.

(19) Corbet, J.-P.; Mignani, G. *Chem. Rev.* **2006**, *106*, 2651−2710.

(20) Upfield shifts for all ring protons of the azulene moiety in **11** were also observed in $CDCl_3$ compared with those of **12**.

(21) The B3LYP/6-31G** time-dependent density functional calculations were performed with *Spartan'10*, Wavefunction: Irvine, CA.

(22) (a) Amir, E.; Amir, R. J.; Campos, L. M.; Hawker, C. J. *J. Am. Chem. Soc.* **2011**, *133*, 10046−10049. (b) Koch, M.; Blacque, O.; Venkatesan, K. *Org. Lett.* **2012**, *14*, 1580−1583.

(23) (a) Bendikov, M.; Wudl, F.; Perepichka, D. F. *Chem. Rev.* **2004**, *104*, 4891−4945. (b) Iyoda, M.; Hasegawa, M.; Miyake, Y. *Chem. Rev.* **2004**, *104*, 5085−5113. (c) Jana, A.; Ishida, M.; Kwak, K.; Sung, Y. M.; Kim, D. S.; et al. *Chem. - Eur. J.* **2013**, *19*, 338−349. (d) Lu, X.; Sun, J.; Liu, Y.; Shao, J.; Ma, L.; Zhang, S.; Zhao, J.; Shao, Y.; Zhang, H.-L.; Wang, Z.; Shao, X. *Chem. - Eur. J.* **2014**, *20*, 9650−9656.

(24) (a) Ito, S.; Morita, N. *Eur. J. Org. Chem.* **2009**, *2009*, 4567−4579. (b) Ito, S.; Shoji, T.; Morita, N. *Synlett* **2011**, *2011*, 2279−2298. (c) Shoji, T.; Ito, S.; Toyota, K.; Yasunami, M.; Morita, N. *Chem. - Eur. J.* **2008**, *14*, 8398−8408. (d) Shoji, T.; Higashi, J.; Ito, S.; Okujima, T.; Yasunami, M.; Morita, N. *Chem. - Eur. J.* **2011**, *17*, 5116−5129.

(25) Constant−voltage oxidation and reduction were applied to solutions of these compounds with a platinum mesh as the working electrode and a wire counter electrode in an electrolytic cell of 1 mm thickness. Visible spectra were measured in degassed benzonitrile containing Et_4NClO_4 (0.1 M) as a supporting electrolyte at room temperature under the electrochemical reaction conditions.

(26) Kageyama, T.; Ueno, S.; Takimiya, K.; Aso, Y.; Otsubo, T. *Eur. J. Org. Chem.* **2001**, *2001*, 2983−2987.

DOI: 10.1021/acs.joc.6b02818
J. Org. Chem. 2017, 82, 1657−1665